

Rabi model beyond the rotating-wave approximation: Generation of photons from vacuum through decoherence

T. Werlang,¹ A. V. Dodonov,¹ E. I. Duzzioni,^{2,*} and C. J. Villas-Bôas¹

¹*Departamento de Física, Universidade Federal de São Carlos, P.O. Box 676, São Carlos, 13565-905, São Paulo, Brazil*

²*Centro de Ciências Naturais e Humanas, Universidade Federal do ABC,*

Rua Santa Adélia, 166, Santo André, São Paulo, 09210-170, Brazil

(Received 5 July 2008; published 5 November 2008)

We study numerically the dynamics of the Rabi Hamiltonian, which describes the interaction of a single cavity mode and a two-level atom without the rotating wave approximation. We analyze this system subjected to damping and dephasing reservoirs, included via the usual Lindblad superoperators in the master equation. We show that the combination of the antirotating term and the atomic dephasing leads to linear asymptotic photon generation from the vacuum. We reveal the origins of the phenomenon and estimate its importance in realistic situations.

DOI: [10.1103/PhysRevA.78.053805](https://doi.org/10.1103/PhysRevA.78.053805)

PACS number(s): 42.50.Pq, 42.50.Ct, 03.65.Yz

I. INTRODUCTION

A fundamental task in physics is the description of the matter-light interaction. The simplest model to deal with this is the Rabi model [1], which describes the interaction of a two-level atom with a single mode of the quantized electromagnetic (EM) field. The Rabi Hamiltonian (RH) reads ($\hbar=1$)

$$H = \omega a^\dagger a + \frac{\omega_0}{2} \sigma_z + g(\sigma_+ + \sigma_-)(a + a^\dagger), \quad (1)$$

where ω and ω_0 are the field and atomic transition frequencies, respectively, and g is the coupling constant (vacuum Rabi frequency). a (a^\dagger) is the annihilation (creation) operator of the EM field, while $\sigma_z = |e\rangle\langle e| - |g\rangle\langle g|$, $\sigma_+ = |e\rangle\langle g|$ and $\sigma_- = \sigma_+^\dagger$ are atomic operators, where $|g\rangle$ and $|e\rangle$ denote the ground and excited atomic states, respectively. Although widely studied over the last few decades, up to now an exact analytical solution is lacking and only numerical [2–5] and approximate analytical solutions are available [6–8], despite the conjecture by Reik and Doucha [9] that an exact solution of RH in terms of known functions is possible. The commonest analytical approach to solving RH is to make use of the rotating wave approximation (RWA), where the antirotating term $g(a^\dagger\sigma_+ + a\sigma_-)$ is neglected. This approximation is widely used because, in the weak coupling regime ($g/\omega \ll 1$), with small detuning $|\Delta| \ll \omega$ ($\Delta = \omega_0 - \omega$) and weak field amplitude, the contribution of this term to the evolution of the system is quite small [10,11]. In this limit, the RH is known as Jaynes-Cummings Hamiltonian (JCH) [12,13] and can be integrated exactly.

For having an exact solution, the JCH has been widely employed in quantum optics, in particular in cavity quantum electrodynamics (QED) [14,15], where the vast majority of experiments satisfy the required parameter regime [10,11].

JCH has revealed interesting phenomena related to the quantum nature of the light, encompassing the granular nature of the electromagnetic field, revealed through collapse and revival of the atomic inversion [16], Rabi oscillations [17], squeezing [18], nonclassical states, such as the Schrödinger catlike state [19] and Fock states [20], and the atom-atom or atom-field entanglement [21]. The manipulation of atom-field interaction has been employed in the implementation of quantum logic gates in trapped ions [22] and in cavity QED [23], as well as the atomic teleportation process [24], which have contributed to a fast development of quantum information science [25]. Moreover, over the past few years the JCH has been investigated experimentally in solid-state cavity QED systems in the strong coupling limit, using superconducting artificial two-level atoms coupled to microwave waveguide resonators [26–28] (the so-called circuit QED [29]) and quantum dots coupled to photonic crystal microcavities [30,31]. In fact, in circuit QED the JCH is the basic theoretical tool for describing quantum logic gates and read-out protocols [32,33].

The antirotating term neglected under RWA is usually wrongly interpreted as being non-conservative [10,11,34], since it could allow for a violation of energy conservation. In fact, this term does not conserve the total number of quanta of the system, defined by the operator $N \equiv a^\dagger a + \sigma_z + \mathbb{I}$ (where \mathbb{I} stands for the identity operator). However, it does not change the total energy of the system, as can easily be seen through the Heisenberg equation of motion for the total Hamiltonian operator $dH/dt = i[H, H] + \partial H/\partial t = 0$, since H in Eq. (1) is time independent. Therefore, the total energy of the system $\langle H \rangle$ is conserved and no violation of physical laws occurs. In addition, recent papers have questioned the validity of the RWA [35–37] and proposed alternative analytical approximate methods [6,8]. Moreover, it has been shown that the antirotating term is responsible for several novel quantum-mechanical phenomena, such as quantum irreversibility and chaos [38,39], quantum phase transitions [40], implementation of Landau-Zener transitions of a qubit in circuit QED architecture [41,42], generation of atom-cavity entanglement [43,44], and simulation of the dynamical Casimir effect (DCE [45]) in semiconducting microcavities [46–48] or circuit QED [44].

*Present address: Instituto de Física, Universidade Federal de Uberlândia, Av. João Naves de Ávila, 2121, Santa Mônica, 38400-902, Uberlândia, MG, Brazil.

Here we study numerically the dynamics of the RH subjected to dissipative effects acting on both the atom and the cavity mode. These undesirable effects are taken into account through the master equation approach [10], where the Lindblad superoperators are built as usual [49]. Without any formal proof, we simply assume that the evolution of the density operator of the system $\rho(t)$ is described by the master equation

$$\frac{\partial \rho}{\partial t} = -i[H, \rho] + \mathcal{L}(\rho), \quad (2)$$

where H is the RH (1) and the Lindblad operator $\mathcal{L}(\rho)$ is given by

$$\mathcal{L}(\rho) = \mathcal{L}_a(\rho) + \mathcal{L}_d(\rho) + \mathcal{L}_f(\rho), \quad (3)$$

with the standard definitions

$$\begin{aligned} \mathcal{L}_a(\rho) = & \frac{\gamma}{2}(n_t + 1)(2\sigma_- \rho \sigma_+ - \sigma_+ \sigma_- \rho - \rho \sigma_+ \sigma_-) \\ & + \frac{\gamma}{2}n_t(2\sigma_+ \rho \sigma_- - \sigma_- \sigma_+ \rho - \rho \sigma_- \sigma_+), \end{aligned} \quad (4)$$

$$\begin{aligned} \mathcal{L}_f(\rho) = & \frac{\kappa}{2}(n_t + 1)(2a\rho a^\dagger - a^\dagger a \rho - \rho a^\dagger a) \\ & + \frac{\kappa}{2}n_t(2a^\dagger \rho a - a a^\dagger \rho - \rho a a^\dagger), \end{aligned} \quad (5)$$

$$\mathcal{L}_d(\rho) = \gamma_{\text{ph}}(\sigma_z \rho \sigma_z - \rho). \quad (6)$$

The superoperators $\mathcal{L}_a(\rho)$ and $\mathcal{L}_f(\rho)$ describe effects of the thermal reservoirs (with mean photon number n_t) on the atom and the field, respectively, where γ (κ) is the atom (cavity) relaxation rate. Another source of decoherence of the atom is the phase damping reservoir, represented by $\mathcal{L}_d(\rho)$, where γ_{ph} is the dephasing rate.

Focusing our attention on asymptotic photon creation from vacuum driven by the combination of the antirotating term $g(a^\dagger \sigma_+ + a \sigma_-)$ in Eq. (1) and the atomic phase reservoir, we show that even in situations where the atom and the field are initially prepared in their individual ground states, i.e., $|\phi\rangle = |g, 0\rangle$, where $|0\rangle$ is the ground state of the EM field, asymptotic photon generation still occurs. This process depends on the intensity of the atom-field coupling g , the detuning Δ , and is considerably amplified when the atomic phase reservoir predominates over the other dissipative channels, such as atomic and field damping due to the thermal reservoirs. The essence of the photon creation mechanism presented here relies on the existence of the antirotating term in the RH and the limitation imposed by the quantum vacuum, namely, $a|0\rangle = 0$. The role played by the atomic phase reservoir is just to amplify the photon creation process through atomic decoherence. As far as we know, this phenomenon has not been described previously in the literature.

This paper is organized as follows. In Sec. II we study in detail the process of photon generation due to atomic dephasing and explain its origin. In Sec. III we give an alternative physical explanation of photon generation by taking the

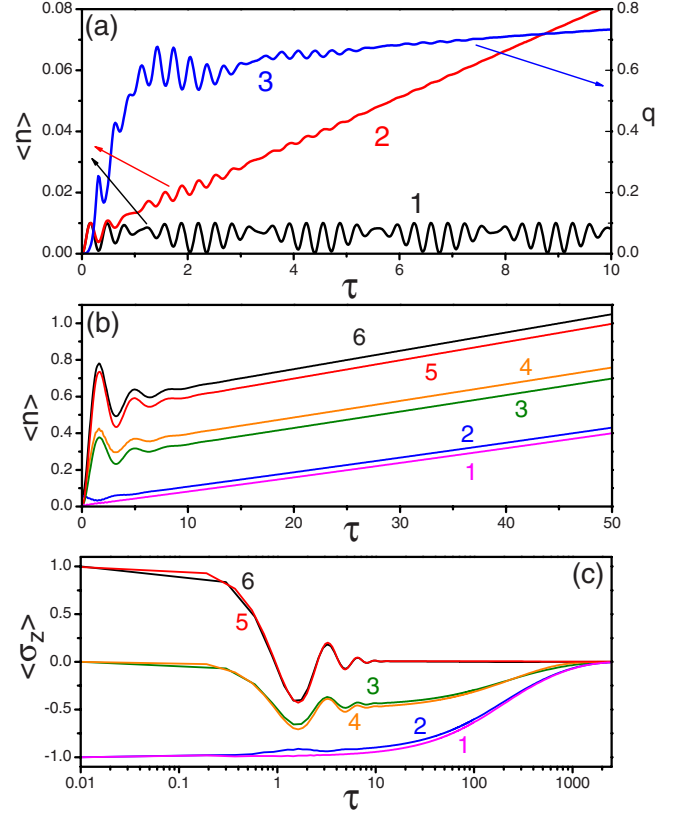


FIG. 1. (Color online) Dynamics of the Rabi Hamiltonian for $\Delta=0$ and $g=0.1$ as a function of dimensionless time $\tau=\xi t$ ($\xi=0.1$). (a) Mean photon number $\langle n \rangle$ for initial state $|g, 0\rangle$ without dephasing (line 1) and with dephasing $\gamma_{\text{ph}}=0.1$ (line 2). Line 2 shows photon generation from the vacuum due to atomic dephasing and the created field state is superpoissonian, since the Mandel factor $q > 0$ (line 3). (b) $\langle n \rangle$ for different initial states $|\phi_i\rangle$, $i=1, \dots, 6$ (see the text), demonstrating that the asymptotic photon generation does not depend on the initial state. (c) Population inversion $\langle \sigma_z \rangle$ for the states $|\phi_i\rangle$ shown in (b): as expected, $\langle \sigma_z \rangle$ goes to zero asymptotically due to the atomic decoherence.

atomic dephasing to be due to random shifts of the atomic transition frequency, as usually occurs in solid state systems (e.g., circuit QED). In Sec. IV we study the influence of the damping process on the photon creation through decoherence and estimate the net effect in realistic situations. Finally, Sec. V contains a discussion of results and concluding remarks.

II. PURE DEPHASING

For convenience, from now on we set the cavity frequency to $\omega=1$. First we integrate Eq. (2) numerically, assuming there is only the dephasing reservoir ($\gamma=\kappa=0$). In Figs. 1 and 2 we set the parameters $\Delta=0$ and $g=0.1$. These and other parameter values have been chosen in order to optimize the numerical calculations, and are not related to experimental data; nevertheless, we verified that qualitatively the behavior described below also holds for realistic parameters [see Fig. 5(b)]. The state $|g, 0\rangle$ is the ground state of the JCH, so it is not coupled to other states under the JCH dynamics. On the other hand, the antirotating term in the RH

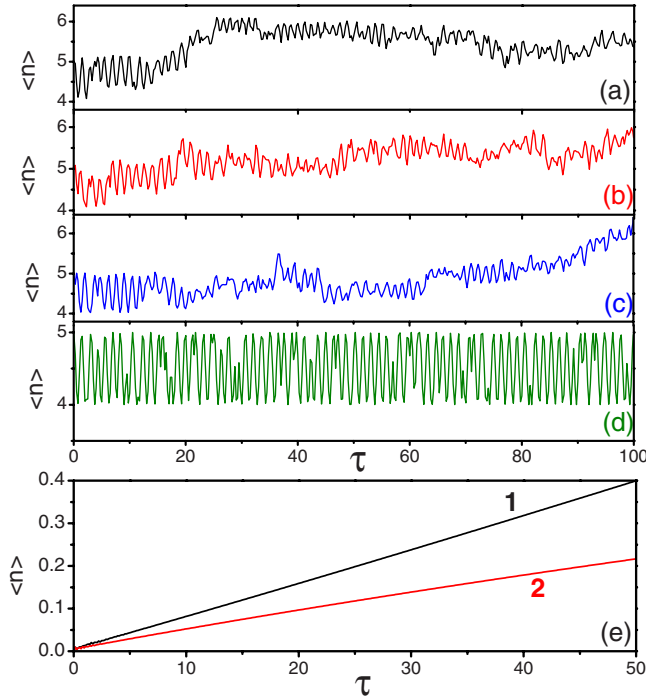


FIG. 2. (Color online) (a)–(c) Mean photon number for RH $\langle n \rangle$ vs τ for three particular trajectories, obtained using the quantum trajectories approach. The parameters are $\Delta=0$, $g=0.1$, $\gamma_{\text{ph}}=0.1$, and the initial state is $|g, 5\rangle$. $\langle n \rangle$ tends to increase with time. (d) $\langle n \rangle$ for a single trajectory using JCH, showing that there is no increase in the photon number without the antirotating term. (e) Asymptotic increase of mean photon number for the RH (line 1) and the test Hamiltonian H_E (line 2, see text), demonstrating that the phenomenon is due to the antirotating term and the limitation by vacuum, $a|0\rangle=0$.

does induce transitions to other states and, since the lower limit of the atom and field states are $|g\rangle$ and $|0\rangle$, respectively, these transitions may only increase $\langle n \rangle$. In Fig. 1(a) we plot the mean photon number $\langle n \rangle$ without dephasing ($\gamma_{\text{ph}}=0$, line 1) as a function of the dimensionless time $\tau \equiv \xi t$, with $\xi = 0.1$ for the initial state $|g, 0\rangle$, showing a bound oscillating behavior, as described in detail in Ref. [3]. Figure 1(a) also shows $\langle n \rangle$ (line 2) and the Mandel factor $q = (\langle \Delta n \rangle^2 - \langle n \rangle) / \langle n \rangle$ (line 3) for a dephasing rate $\gamma_{\text{ph}}=0.1$; now $\langle n \rangle$ increases with time, tending asymptotically to a linear rate of increase, and the generated field state demonstrates a super-Poissonian behavior $q > 0$.

The photon creation mechanism through atomic dephasing demonstrated in Fig. 1(a) is a general phenomenon whose asymptotic limit does not depend on the initial state of the system. In Fig. 1(b) we plot $\langle n \rangle$ vs τ for six different initial states: $|\phi_1\rangle = |g, 0\rangle$, $|\phi_2\rangle = |g, \alpha\rangle$, where $|\alpha\rangle$ is the coherent state and we take $|\alpha|^2 = 0.05$, $|\phi_3\rangle = [(|g\rangle + |e\rangle) / \sqrt{2}] \otimes |0\rangle$, $|\phi_4\rangle = [(|g\rangle + |e\rangle) / \sqrt{2}] \otimes |\alpha\rangle$, $|\phi_5\rangle = |e, 0\rangle$, and $|\phi_6\rangle = |e, \alpha\rangle$. The basic difference between these initial states is the number of quanta $\langle N_k \rangle = \langle \phi_k | N | \phi_k \rangle$: we have $\langle N_1 \rangle = 0$, $\langle N_2 \rangle = 0.05$, $\langle N_3 \rangle = 0.5$, $\langle N_4 \rangle = 0.55$, $\langle N_5 \rangle = 1$, and $\langle N_6 \rangle = 1.05$. We see that after the transient regime ($\tau \geq 15$), whose duration is proportional to the initial number of quanta, all curves show the same behavior—a linear time dependence with the same photon

creation rate. In Fig. 1(c) we plot the atomic population inversion $\langle \sigma_z \rangle$ for these states, showing that asymptotically $\langle \sigma_z \rangle$ approaches zero for any initial state. This result is expected, owing to atomic decoherence.

The master equation describes only the net effect of the environment on the system. For a better understanding of the role played by the atomic dephasing on the creation of photons we use the quantum trajectories approach [49,50] to study $\langle n \rangle$ during individual trajectories. Here the quantum jump operator is $J\rho = \gamma_{\text{ph}}\sigma_z\rho\sigma_z$ and the non-Hermitian Hamiltonian is $\tilde{H} = H - i(\gamma_{\text{ph}}/2)\mathbb{I}$. In Figs. 2(a)–2(c) we plot $\langle n \rangle$ vs τ for three samples of individual trajectories for the initial number state $|g, 5\rangle$; note that in each trajectory, $\langle n \rangle$ tends to increase as the time goes on. This occurs for two reasons: (i) the antirotating term in RH and (ii) the limitation of the cavity field from below by the vacuum $a|0\rangle=0$.

To illustrate (i), in Fig. 2(d) we plot $\langle n \rangle$, obtained by the quantum trajectories approach for the JCH under atomic dephasing, where we see that $\langle n \rangle$ oscillates with time but does not increase, in contrast to Figs. 2(a)–2(c). To explain the process of photon creation, we notice that any state may be written in terms of the basis states $\{|s, n\rangle\}$ (with $s = \{g, e\}$ and $|n\rangle$ the Fock state). Between the jumps, the system evolves according to the Rabi Hamiltonian (1) (the non-Hermitian part is not important due to the normalization condition [51]). The JCH promotes $|g, n\rangle \leftrightarrow |e, n-1\rangle$ transitions, while the antirotating term induces $|g, n\rangle \leftrightarrow |e, n+1\rangle$. The combined action of both parts generates all the possible transitions. However, the Fock states are limited from below by the vacuum state (ii), so there are more available $|s, m > n\rangle$ than $|s, m < n\rangle$ states and the mean number of photons between the jumps tends to increase. Upon a jump, the reservoir “reads out” the atomic state through the application of $\sqrt{\gamma_{\text{ph}}}\sigma_z$ to the wave function, which transforms $|g\rangle \rightarrow -\sqrt{\gamma_{\text{ph}}}|g\rangle$ and $|e\rangle \rightarrow \sqrt{\gamma_{\text{ph}}}|e\rangle$. Thus, the coherence between the states $|g\rangle$ and $|e\rangle$ is lost and subsequent evolution under H will not bring the system back to the state at the moment of the previous jump. For this reason, after each jump, $\langle n \rangle$ tends to be larger than upon the last jump, as clearly demonstrated in Figs. 2(a)–2(c). After taking a statistical average over many trajectories one finds out that $\langle n \rangle$ always increases, in agreement with Fig. 1.

One might suspect a third explanation for photon generation due to atomic dephasing—the different weights \sqrt{n} and $\sqrt{n+1}$ arising upon applying a and a^\dagger to the Fock state $|n\rangle$. To show that this is not the case we consider the test Hamiltonian H_E obtained by replacing the operators a and a^\dagger in RH (1) with the exponential phase operators [52,53] $E_- \equiv (n+1)^{-1/2}a$ and $E_+ = E_-^\dagger$, respectively, where $E_+E_- = \mathbb{I} - |0\rangle\langle 0|$. By doing this we eliminate the weight factors \sqrt{n} and $\sqrt{n+1}$ from the RH, since $E_+|n\rangle = |n+1\rangle$ and $E_-|n\rangle = (1 - \delta_{n0})|n-1\rangle$. In Fig. 2(e) we plot $\langle n \rangle$ for RH (line 1) and $\langle n_E \rangle$, obtained from H_E (line 2), against τ for initial state $|\phi\rangle = |g, 0\rangle$. In both cases there is photon creation from vacuum, although $\langle n_E \rangle$ increases more slowly than $\langle n \rangle$. Therefore this photon creation phenomenon is not due to the different weights \sqrt{n} and $\sqrt{n+1}$ attributed to the operators a and a^\dagger , but to the presence of the EM vacuum state.

From Fig. 1 we note that in the asymptotic limit $\langle n(\tau) \rangle$ increases linearly with time, so a deeper insight into the

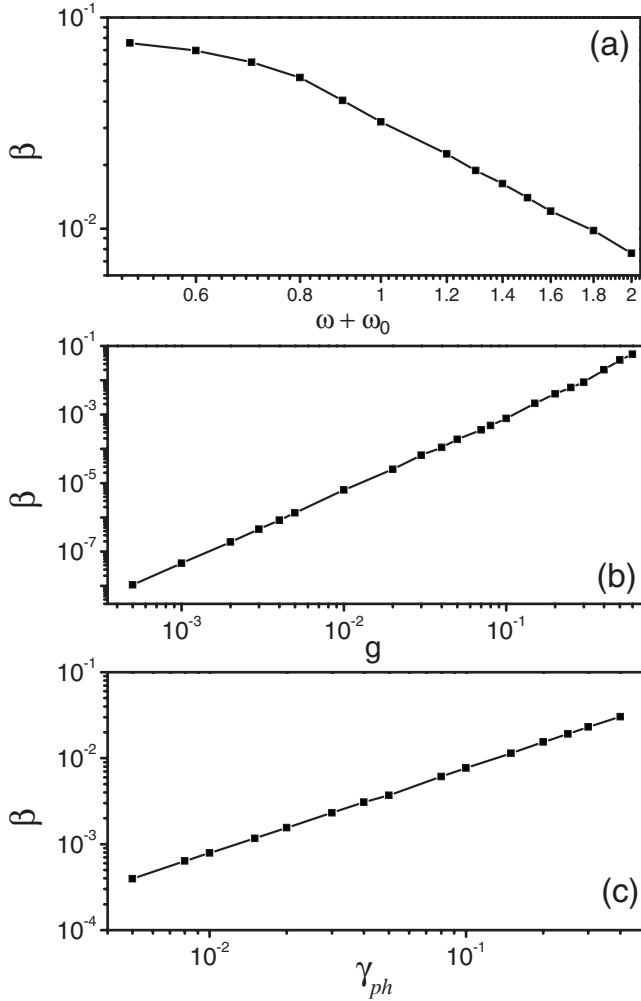


FIG. 3. Variation of asymptotic photon generation rate $\beta \equiv d\langle n(\tau) \rangle / d\tau|_{as}$ with (a) $(\omega + \omega_0)$ for fixed g and γ_{ph} ; (b) g for fixed γ_{ph} and ω_0 ; (c) γ_{ph} for fixed g and ω_0 . We observe that $\beta \sim \gamma_{ph}$ and is inversely proportional to $(\omega + \omega_0)^2$. In the weak coupling regime $\beta \sim g^2$.

problem can be gained by analyzing how the asymptotic photon generation rate $\beta \equiv d\langle n(\tau) \rangle / d\tau|_{as}$ scales with $\omega + \omega_0$, g , and γ_{ph} (here we fix ω and vary the other parameters). In Fig. 3(a), we plot β vs $(\omega + \omega_0)$, for fixed g and γ_{ph} , and we see that β increases as ω_0 decreases, so β is inversely proportional to $(\omega + \omega_0)^2$. Figure 3(b) shows the dependence of β on g (up to $g=1$) for fixed γ_{ph} and ω_0 : for $g \ll 1$ (the weak coupling regime) analysis of the curve shows that $\beta \sim g^2$, although this dependence is modified for larger values of g . Finally, Fig. 3(c) shows that $\beta \sim \gamma_{ph}$ for fixed g and ω_0 , in agreement with the quantum trajectories approach: indeed, a larger γ_{ph} implies a greater jump probability and, consequently, on average $\langle n \rangle$ increases at a faster rate. A quantitative analysis of β will be presented elsewhere [54].

III. RANDOM FREQUENCY FLUCTUATIONS

One of the origins of dephasing from a physical point of view are the random shifts of the atomic transition frequency

ω_0 due to interaction with the environment [49,55]. Indeed, $1/f$ noise in the bias controlling the atomic transition frequency is the dominant source of decoherence in superconducting artificial atoms (qubits) [32,56–58]. To investigate the effect of such noise on the dynamics of the atom-cavity system, we integrated numerically the master equation (2) for the RH (with $\gamma = \kappa = \gamma_{ph} = 0$), assuming that ω_0 has stochastic fluctuations. Our goal was to show that, when averaged over the ensemble, this source of decoherence does generate photons from the vacuum, since its mathematical description can be given by the dephasing Lindblad superoperator in the master equation we studied above.

As a simple model we considered time-dependent $\omega_0(t)$

$$\omega_0(t+dt) = \omega_0(t) + \begin{cases} 0.1\epsilon xr & \text{if } \omega_0(t) < \Omega_0 - 0.8\epsilon, \\ -0.1\epsilon xr & \text{if } \omega_0(t) > \Omega_0 + 0.8\epsilon, \\ 0.1\epsilon x(r-1/2) & \text{otherwise,} \end{cases} \quad (7)$$

where $\Omega_0 \equiv \omega_0(t=0)$ is the mean atomic transition frequency $r \in (0, 1)$ is a random number, $\epsilon \ll 1$ is the maximum shift of the atom frequency and dt is the simulation unit step, $gdt \ll 1$. Here x is related to the “frequency” of the noise: qualitatively, for small x (see discussion below) we have “low frequency” noise, and at the opposite limit we have “high frequency” noise.

We assumed the initial state $|g, 0\rangle$ and calculated the ensemble average of the mean photon number $\langle n \rangle_{av}$ and the probability of exciting the atom P_e , adopting the parameters $\Omega_0 = 1$, $g = 6 \times 10^{-2}$, $\epsilon = g$. We considered three examples of noise whose spectra are shown in Fig. 4(a): $x=1$ corresponds to the “low-frequency” noise (line 1) and $x=6$ is our reference to the “high-frequency” noise (line 3), while $x=3$ is a case in between that we call “middle frequency” noise [line 2, data not shown in Fig. 1(a) since it lies between lines 1 and 3]. First, Fig. 4(b) shows three samples of $\langle n \rangle$ obtained for single simulation runs for the “high frequency” noise—random rises and falls of photon number can be seen, but on average $\langle n \rangle$ increases. Figures 4(c) and 4(d) show $\langle n \rangle_{av}$ and P_e , respectively, obtained after averaging out many simulation runs for the three kinds of noise. We see that on average there is a growth of both $\langle n \rangle_{av}$ and P_e ; moreover, the growth of $\langle n \rangle_{av}$ is approximately linear in time, in agreement with our previous results.

From Fig. 4(c) we see that the photon generation rate is higher for higher frequency noise. One may understand qualitatively such behavior as follows. The dynamics of the RH with externally prescribed nonrandom $\omega_0(t)$ allows for the coherent generation of both EM and atomic real excitations from the vacuum, for example, in the case of periodic [44,46–48] or linear [41,43] time dependence of $\omega_0(t)$. Moreover, the photon creation rate strongly depends on the shape of $\omega_0(t)$ [41] and, in the periodic case, on the periodicity of the modulation of $\omega_0(t)$ [44,46]. The Fourier transform [Fig. 4(a)] of the noise contains the “resonant” frequencies ($\nu \sim 2$ [44,46]), with respective weights, for which photon generation occurs in the periodic case, so on average one expects a slow incoherent photon creation from vacuum due to these components in the noise spectrum. For the high

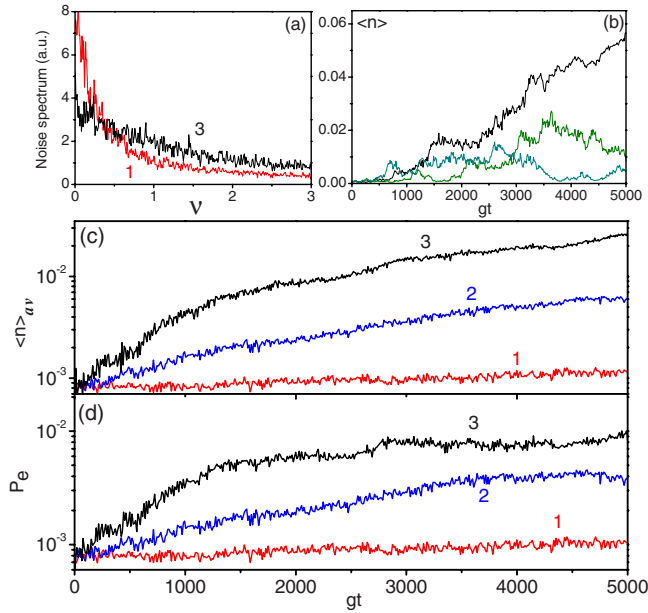


FIG. 4. (Color online) Simulation of atomic dephasing via random atomic frequency fluctuations for parameters $\Omega_0=1$, $g=6 \times 10^{-2}$, $\varepsilon=g$. (a) Spectrum of the frequency noise $\omega_0(t)-\Omega_0$. Line 1 (red) corresponds to the “low-” and line 3 (black) to the “high-” frequency noise. (b) $\langle n \rangle$ for three individual simulation runs using high frequency noise. (c) $\langle n \rangle_{av}$ averaged out over many simulation runs, showing photon growth, dependent on the noise frequency. Here line 2 (blue) is the “middle-frequency” noise. (d) P_e averaged out over many simulations. These curves agree qualitatively with the results obtained above using the master equation approach.

frequency noise, there are more resonant frequencies in the noise spectrum and/or their weight is larger compared to the low-frequency noise, so the photon growth rate is higher, in agreement with Fig. 4(c). Therefore, one of the physical origins of photon creation through decoherence in cavity QED are random fluctuations of the atomic transition frequency giving rise to an effective time-dependent RH, for which photons are created from the vacuum for the “resonant” frequencies [44,46] present in the noise spectrum.

IV. DEPHASING PLUS RELAXATION

In realistic situations, in addition to the dephasing reservoir there are other important error sources (environments) acting on the system, e.g., thermal reservoirs. When other reservoirs are present, there is a competition between photon creation due to the atomic dephasing and photon loss due to the damping. In order to see this effect, in Fig. 5(a) we plot $\langle n \rangle$ vs τ for different decay rates in Eq. (2), for the parameters $\Delta=0$, $g=0.1$, $n_t=0$, and the initial state $|g, 0\rangle$. The effect of temperature ($n_t > 0$) is just to shift the curves upward. When the atomic phase reservoir is switched off, curve 1, with dissipation parameters $(0, 0, 1) \times 10^{-1}$ [we use notation $(\gamma_{ph}, \gamma, \kappa)$], and 2, with $(0, 1, 0) \times 10^{-1}$, show that at large times $\langle n \rangle$ is smaller than in the cases where the phase reservoir is switched on, as shown in the curves 3 with $(1, 1, 1) \times 10^{-1}$, 4 with $(1, 0, 1) \times 10^{-1}$, and 5 with $(1, 1, 0) \times 10^{-1}$.

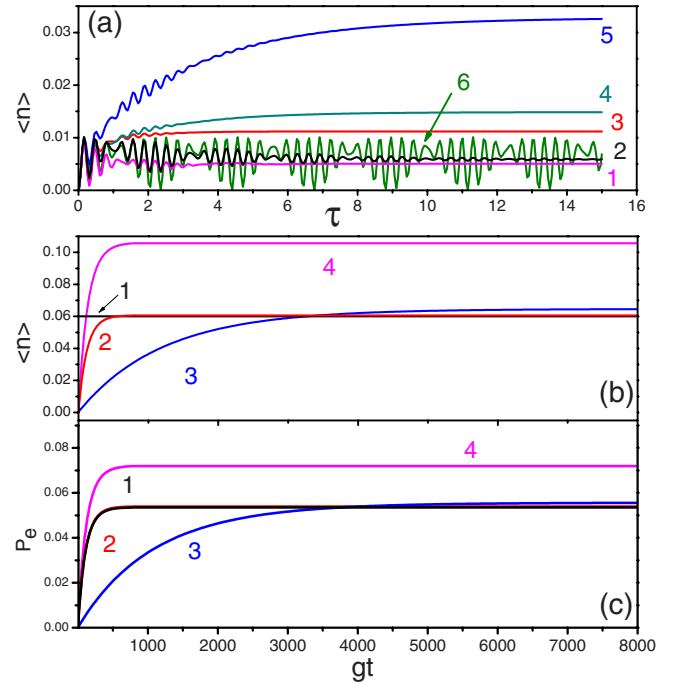


FIG. 5. (Color online) (a) $\langle n \rangle$ vs τ using the master equation (2) for initial state $|g, 0\rangle$ with parameters $\Delta=0$, $g=0.1$, $n_t=0$ and decay rates $(\gamma_{ph}, \gamma, \kappa)$ as follows. Line 1: $(0, 0, 1) \times 10^{-1}$, line 2: $(0, 1, 0) \times 10^{-1}$, line 3: $(1, 1, 1) \times 10^{-1}$, line 4: $(1, 0, 1) \times 10^{-1}$, line 5: $(1, 1, 0) \times 10^{-1}$, line 6: $(0, 0, 0)$. (b) $\langle n \rangle$ vs gt for initial state $|g, 0\rangle$ using circuit QED parameters $\Delta=0$, $g=2 \times 10^{-2}$, $n_t=6 \times 10^{-2}$ and distinct decay rates (line 1 denotes the thermal photon number n_t). Line 2: current parameters $(2, 3, 0.4) \times 10^{-4}$. Line 3: expected future scenario $(2, 3, 0.4) \times 10^{-5}$. Line 4: highly biased noise $(200, 3, 0.4) \times 10^{-4}$. For current parameters there is no observable difference between n_t and $\langle n \rangle$, however, in the future or in a very noisy environment $\langle n \rangle$ may become significantly larger than n_t due to photon creation through decoherence. (c) P_e corresponding to the parameters in (b); P_e resembles the behavior of $\langle n \rangle$.

Line 6 shows $\langle n \rangle$ in the absence of any reservoir. Even in situations in which the environment starts at $T=0$ K, in the asymptotic limit the system behaves as if subjected to an effective reservoir with $\bar{n}_t > 0$, since $\lim_{\tau \rightarrow \infty} \langle n(\tau) \rangle > 0$. The number of effective reservoir photons \bar{n}_t increases when the atomic phase reservoir is present (see curves 3, 4, and 5) and decreases when the atomic and field thermal reservoirs are predominant. However, the effective reservoir cannot be compared to the usual thermal reservoir, since the statistics of the created field state is quite different from the thermal state statistics. A similar conclusion was drawn in Ref. [35], where the authors considered the master equation (2) at zero temperature with $\gamma_{ph}=\gamma=0$, $\kappa \neq 0$ and showed that the anti-rotating part of the RH gives rise to a thermal-like term in the effective master equation, although it cannot be interpreted as an interaction with a thermal bath at a certain temperature.

In Fig. 5(b) we consider current experimental parameters taken from recent circuit QED experiments [59]: $\Delta=0$, $g=2 \times 10^{-2}$, $n_t=6 \times 10^{-2}$. Line 1 shows the thermal photon number n_t and line 2 shows $\langle n \rangle$ obtained via master equation (2) for present-day dissipation rates: $\kappa=4 \times 10^{-5}$, $\gamma=3$

$\times 10^{-4}$, $\gamma_{\text{ph}}=2 \times 10^{-4}$. There is no visible deviation of $\langle n \rangle$ from n_t for the currently available temperatures, even if the detuning is increased to $\Delta=-0.2$ (data not shown). Next we consider the scenario expected in the near future, when damping losses can be suppressed one order of magnitude, $\kappa=4 \times 10^{-6}$, $\gamma=3 \times 10^{-5}$, but the dephasing rate remains the same, $\gamma_{\text{ph}}=2 \times 10^{-4}$. In this case (line 3), $\langle n \rangle$ deviates slightly from the thermal photon number n_t and such an effect could be observed in very accurate measurements. Last, we take the current values of damping rates, $\kappa=4 \times 10^{-5}$, $\gamma=3 \times 10^{-4}$, and consider a highly biased noise [58] with the dephasing rate two order of magnitudes larger than the best one available today, $\gamma_{\text{ph}}=2 \times 10^{-2}$ (line 4). In this case, $\langle n \rangle$ is almost twice the thermal photon number, due to the phenomenon of photon creation through decoherence.

Finally, in Fig. 5(c) we plot P_e corresponding to the parameters of Fig. 5(b), where the line 1 shows P_e^{RWA} obtained for current experimental dissipation parameters using the JCH, which is nearly independent of the relaxation rates. The behavior of P_e resembles that of $\langle n \rangle$, indicating that P_e increases due to the combined action of dephasing and the antirotating term, although for current parameters this phenomenon is insignificant. However, for a large γ_{ph} (line 4) P_e is substantially higher than P_e^{RWA} , demonstrating that large dephasing, in addition to decoherence, may also induce bit flip error.

V. DISCUSSION AND CONCLUDING REMARKS

We studied numerically the dynamics of the Rabi Hamiltonian subjected to dissipative losses, assuming *ad hoc* that one may describe the dissipative dynamics of the RH by using the standard master equation with usual damping and dephasing Lindblad superoperators. We found out that the atomic dephasing, when combined with the antirotating term in the RH, induces photon creation from the vacuum. A physical interpretation of this phenomenon was given, by

adopting two alternative approaches: (1) the quantum trajectories approach based on quantum jumps and (2) microscopic *ad hoc* model of dephasing based on stochastic oscillations of the atomic transition frequency (as occurs in solid state cavity QED). We showed that the photon creation through atomic decoherence is suppressed in the presence of damping mechanisms, and estimated the magnitude of this phenomenon using current experimental values of parameters, noting that the phenomenon might become relevant in future experiments.

Although we did not present a formal deduction of the master equation (2) we used throughout this treatment, we can ensure its validity for the Rabi Hamiltonian in the weak atom-field coupling regime ($g \ll \omega, \omega_0$) based on recent experiments in circuit QED [27,59], where the experimental results agree with the master equation description used above [33,60]. Moreover, as discussed in Sec. III, our results obtained through numerical simulation of random frequency fluctuations agree qualitatively with the master equation approach. Thus, we believe that the results obtained here are important because they show that decoherence induces photon generation from the vacuum, and that such an effect may become relevant in future experiments with lower temperatures and lower damping rates. Finally, we stress that further investigation of the problem is needed, since up to now the theoretical and numerical research has mainly focused on the role of the RH antirotating term in closed system dynamics, while our study points to important new effects of the antirotating term in open systems.

ACKNOWLEDGMENTS

The authors would like to thank the Brazilian agencies CNPq (T.W. and C.J.V-B), FAPESP Grant No. 04/13705-3 (A.V.D.) and UFABC (E.I.D.). This work was supported by Brazilian Millennium Institute for Quantum Information and FAPESP Grant No. 2005/04105-5.

-
- [1] I. I. Rabi, Phys. Rev. **49**, 324 (1936); **51**, 652 (1937).
 - [2] C. Emary, Int. J. Mod. Phys. B **17**, 5477 (2003).
 - [3] R. F. Bishop and C. Emary, J. Phys. A **34**, 5635 (2001).
 - [4] R. F. Bishop *et al.*, Phys. Lett. A **254**, 215 (1999); R. F. Bishop, N. J. Davidson, R. M. Quick, and D. M. van der Walt, Phys. Rev. A **54**, R4657 (1996).
 - [5] V. Fessatidis, J. D. Mancini, and S. P. Bowen, Phys. Lett. A **297**, 100 (2002).
 - [6] A. Pereverzev and E. R. Bittner, Phys. Chem. Chem. Phys. **8**, 1378 (2006).
 - [7] N. Debergh and A. B. Klimov, Int. J. Mod. Phys. A **16**, 4057 (2001).
 - [8] E. K. Irish, Phys. Rev. Lett. **99**, 173601 (2007).
 - [9] H. G. Reik and M. Doucha, Phys. Rev. Lett. **57**, 787 (1986); H. Reik *et al.*, J. Phys. A **20**, 6327 (1987).
 - [10] M. O. Scully and M. S. Zubairy, *Quantum Optics* (Cambridge University Press, Cambridge, 1997).
 - [11] W. P. Schleich, *Quantum Optics in Phase Space* (Wiley-VCH Verlag, Berlin, 2001).
 - [12] E. T. Jaynes and F. W. Cummings, Proc. IEEE **51**, 89 (1963).
 - [13] B. W. Shore and P. L. Knight, J. Mod. Opt. **40**, 1195 (1993).
 - [14] H. Mabuchi and A. C. Doherty, Science **298**, 1372 (2002).
 - [15] J. M. Raimond, M. Brune, and S. Haroche, Rev. Mod. Phys. **73**, 565 (2001).
 - [16] G. Rempe, H. Walther, and N. Klein, Phys. Rev. Lett. **58**, 353 (1987).
 - [17] M. Brune, F. Schmidt-Kaler, A. Maali, J. Dreyer, E. Hagley, J. M. Raimond, and S. Haroche, Phys. Rev. Lett. **76**, 1800 (1996).
 - [18] J. R. Kuklinski and J. L. Madajczyk, Phys. Rev. A **37**, 3175 (1988).
 - [19] M. Brune, S. Haroche, J. M. Raimond, L. Davidovich, and N. Zagury, Phys. Rev. A **45**, 5193 (1992).
 - [20] M. Weidinger, B. T. H. Varcoe, R. Heerlein, and H. Walther, Phys. Rev. Lett. **82**, 3795 (1999).
 - [21] S. J. D. Phoenix and P. L. Knight, Phys. Rev. A **44**, 6023

- (1991); M. Yönaç, T. Yu, and J. H. Eberly, *J. Phys. B* **39**, S621 (1996).
- [22] J. I. Cirac and P. Zoller, *Phys. Rev. Lett.* **74**, 4091 (1995).
- [23] T. Pellizzari, S. A. Gardiner, J. I. Cirac, and P. Zoller, *Phys. Rev. Lett.* **75**, 3788 (1995); T. Sleator and H. Weinfurter, *ibid.* **74**, 4087 (1995).
- [24] S.-B. Zheng and G.-C. Guo, *Phys. Rev. Lett.* **85**, 2392 (2000); M. D. Barrett *et al.*, *Nature (London)* **429**, 737 (2004).
- [25] M. A. Nielsen and I. L. Chuang, *Quantum Computation and Quantum Information* (Cambridge University Press, Cambridge, 2000).
- [26] I. Chiorescu *et al.*, *Nature (London)* **431**, 159 (2004).
- [27] A. Wallraff *et al.*, *Nature (London)* **431**, 162 (2004).
- [28] J. Johansson, S. Saito, T. Meno, H. Nakano, M. Ueda, K. Semba, and H. Takayanagi, *Phys. Rev. Lett.* **96**, 127006 (2006).
- [29] A. Zagoskin and A. Blais, *Can. J. Phys.* **63**, 215 (2007).
- [30] J. P. Reithmaier *et al.*, *Nature (London)* **432**, 197 (2004).
- [31] T. Yoshie *et al.*, *Nature (London)* **432**, 200 (2004).
- [32] A. Blais, R. S. Huang, A. Wallraff, S. M. Girvin, and R. J. Schoelkopf, *Phys. Rev. A* **69**, 062320 (2004).
- [33] A. Blais, J. Gambetta, A. Wallraff, D. I. Schuster, S. M. Girvin, M. H. Devoret, and R. J. Schoelkopf, *Phys. Rev. A* **75**, 032329 (2007).
- [34] C. Gerry and P. Knight, *Introductory Quantum Optics* (Cambridge University Press, Cambridge, 2005).
- [35] A. B. Klimov, J. L. Romero, and C. Saavedra, *Phys. Rev. A* **64**, 063802 (2001).
- [36] J. Larson, *Phys. Scr.* **76**, 146 (2007).
- [37] G. Berlin and J. Aliaga, *J. Opt. B: Quantum Semiclassical Opt.* **6**, 231 (2004).
- [38] L. Bonci, R. Roncaglia, B. J. West, and P. Grigolini, *Phys. Rev. Lett.* **67**, 2593 (1991).
- [39] C. Emary and T. Brandes, *Phys. Rev. Lett.* **90**, 044101 (2003).
- [40] C. Emary and T. Brandes, *Phys. Rev. E* **67**, 066203 (2003).
- [41] K. Saito *et al.*, *Europhys. Lett.* **76**, 22 (2006).
- [42] K. Saito, M. Wubs, S. Kohler, Y. Kayanuma, and P. Hanggi, *Phys. Rev. B* **75**, 214308 (2007).
- [43] M. Wubs, M. S. Kohler, and P. Hanggi, *Photonics Spectra* **40**, 187 (2007).
- [44] A. V. Dodonov *et al.*, e-print arXiv:0806.4035.
- [45] V. V. Dodonov, *Adv. Chem. Phys.* **119**, 309 (2001).
- [46] C. Ciuti and I. Carusotto, *J. Appl. Phys.* **101**, 081709 (2007).
- [47] S. De Liberato, C. Ciuti, and I. Carusotto, *Phys. Rev. Lett.* **98**, 103602 (2007).
- [48] C. Ciuti, G. Bastard, and I. Carusotto, *Phys. Rev. B* **72**, 115303 (2005).
- [49] H. Carmichael, *An Open System Approach to Quantum Optics* (Springer-Verlag, Berlin, 1993).
- [50] M. B. Plenio and P. L. Knight, *Rev. Mod. Phys.* **70**, 101 (1998).
- [51] H. Goto and K. Ichimura, *Phys. Rev. A* **72**, 054301 (2005).
- [52] F. London, *Z. Phys.* **37**, 915 (1926); **40**, 193 (1927).
- [53] L. Susskind and J. Glogower, *Physics (Long Island City, N.Y.)* **1**, 49 (1964).
- [54] T. Werlang *et al.* (in preparation).
- [55] Y. Makhlin, G. Schön, and A. Shnirman, *Rev. Mod. Phys.* **73**, 357 (2001).
- [56] G. Ithier *et al.*, *Phys. Rev. B* **72**, 134519 (2005).
- [57] P. J. Leek *et al.*, *Science* **318**, 1889 (2007).
- [58] P. Aliferis *et al.*, e-print arXiv:0806.0383.
- [59] D. I. Schuster *et al.*, *Nature (London)* **445**, 515 (2007).
- [60] M. Boissonneault, J. M. Gambetta, and A. Blais, *Phys. Rev. A* **77**, 060305(R) (2008).